

Biochemical and molecular assessment of selenium forms for the alleviation of oxidative stress in senescent human fibroblasts

Hazem K. Ghneim, Mohammad A. Alfihli[✉], Sami O. Alharbi, Shady M. Alhusayni, Manal Abudawood and Yazeed A. Al-Sheikh

Chair of Medical and Molecular Genetics Research, Department of Clinical Laboratory Sciences, College of Applied Medical Sciences, King Saud University, Riyadh, Saudi Arabia

Abstract. Selenium enhances the cellular antioxidant capacity and alleviates oxidative stress. We investigated the transcriptional and enzymatic activities of selenium-dependent glutathione peroxidase 1 and thioredoxin reductase 1 (TrxR1), and levels of glutathione, hydrogen peroxide, lipid peroxides, and protein carbonyls in primary passage 5 (P5) and senescent passage 25 (P25) and 30 (P30) fibroblasts. Cells were incubated in either standard Dulbecco growth medium (CM1) containing normal plasma selenium levels (0.8 $\mu\text{mol/l}$), or in CM2, CM3, and CM4 containing 3 $\mu\text{mol/l}$ (5 $\mu\text{mol/l}$ for TrxR1) sodium selenite, L-hydroxyselenomethionine, or Se-methylselenocysteine, respectively. Gene transcripts and activities of both investigated enzymes as well as the levels of reduced glutathione were significantly increased in CM2-, CM3-, and CM4-incubated senescent P25 and P35 cells compared against those incubated in CM1. In congruence, although all oxidative stress parameters including oxidized glutathione were significantly lower in CM2-, CM3-, and CM4-incubated senescent cells compared against those incubated in CM1, such reductions were of significantly higher magnitude in CM3 and CM4 cells compared against those in CM2. In conclusion, organic L-hydroxyselenomethionine and Se-methylselenocysteine are equally more potent at alleviating oxidative stress in senescent cells than inorganic sodium selenite, and thus could be beneficial for use in elderly subjects and those with oxidative stress-associated disease.

Key words: Senescence — Aging — Oxidative stress — Selenium — Fibroblasts

Abbreviations: CM, culture medium; DNP, dinitrophenyl hydrazine; DTNB, 5,5-dithiobis-2-nitrobenzoic acid; FBS, fetal bovine serum; GP, glycogen phosphorylase; GPx1, glutathione peroxidase 1; GR, glutathione reductase; GSH, reduced glutathione; GSSG, oxidized glutathione; LDH, lactate dehydrogenase; LPO, lipid peroxides; MSC, Se-methylselenocysteine; PCC, protein carbonyl content; PFK, phosphofructokinase; ROS, reactive oxygen species; SA, superoxide anions; SM, L-selenomethionine; SS, sodium selenite; TRxR1, thioredoxin reductase 1.

Electronic supplementary material. The online version of this article (doi: 10.4149/gpb_2022024) contains Supplementary Material.

Correspondence to: Mohammad A. Alfihli, Chair of Medical and Molecular Genetics Research, Department of Clinical Laboratory Sciences, College of Applied Medical Sciences, King Saud University, Riyadh 12372, Saudi Arabia
E-mail: malfeehily@ksu.edu.sa

© The Authors 2022. This is an **open access** article under the terms of the Creative Commons Attribution-NonCommercial 4.0 International License (<https://creativecommons.org/licenses/by-nc/4.0/>), which permits non-commercial use, distribution, and reproduction in any medium, provided the original work is properly cited.

Introduction

Selenium (Se), is a vital cationic mineral element with biological importance. Se is present in different forms in nature. In food there are specific combinations of inorganic and organic Se indicating different bioavailability. These forms are of increasing importance due to their supplementary benefits for the amelioration of oxidative stress (Ferreira et al. 2021). The organic Se forms include selenocysteine and L-selenomethionine (SM) plus their methylated derivatives. SM is available in plant and animal products, whereas selenocysteine is mostly present in animal-derived food, and Se-methylselenocysteine (MSC) is the natural predominant form found in some vegetables, namely the alums and brassia (Qazi et al. 2019; Kim et al. 2020). Inorganic selenite and selenate salts mostly originate in vegetables and shell-fish (Qazi et al. 2019). These Se forms are present in soils and are both absorbed by plants and transformed into selenocysteine, SM and their methylated forms, and are all used for biofortification of vegetables (Schiavon and Pilon-Smits 2017). Even though SM cannot be synthesized in humans, it is the most abundant Se form accounting for ~45% of total body Se (Kieliszek 2019). It is acquired from the diet and has the highest rate of gastrointestinal absorption compared to other Se compounds (Kieliszek and Blazejak 2016). Selenoprotein biosynthesis has an indispensable role in maintaining the homeostatic redox state (Huang et al. 2015), and is influenced by Se intake (Legrain et al. 2014).

In selenoproteins, Se exists as selenocysteine (Kieliszek 2019). Thus far, around thirty selenoproteins have been identified, many of which exhibit enzymatic activity (Labunskyy et al. 2014). Se deficiency and selenoproteins are linked to a large number of human pathologies including musculoskeletal disorders, cardiovascular disease, hepatopathies, renal failure, neurologic disorders, cancer, immune and inflammatory disorder, diabetes mellitus, endocrine disorders, and age-related disorders (Kieliszek et al. 2022).

Prominent examples of selenoproteins include glutathione peroxidase 1 (GPx1) and thioredoxin reductase 1 (TrxR1). The GPx family is comprised of eight isoforms, five of which (GPx 1, 2, 3, 4 and 6) are selenoproteins that incorporate a selenocysteine residue at their catalytic center (Gouriprasanna Roy 2005). GPx1 is ubiquitous, most abundantly expressed and is located in the cytoplasm and mitochondria. It reacts with reduced glutathione (GSH) as a substrate for the reduction of hydrogen peroxide (H_2O_2) and organic hydroperoxides (Gromer et al. 2005), thus protecting against DNA and cell membrane damage, and oxidation of hemoglobin and fatty acids (Kieliszek et al. 2018). While in RNA, levels of several selenoproteins, such as type 1 iodothyronine deiodinase and selenoprotein P, are not affected by Se deficiency. Cellular GPx1 expression is rapidly blunted when Se supply is low and its activity is restored upon Se supplementation (Ghneim and Al-Sheikh 2011). TrxR is an antioxidant flavo-

protein that supplies reduced thioredoxin to inhibit apoptosis and reduce hydroperoxides, lipid peroxides, oxidized glutathione (GSSG), H_2O_2 , and dehydroascorbate (Kieliszek et al. 2019). The enzyme has three isoforms; cytosolic TrxR1 and mitochondrial TrxR2 and TrxR3 which are predominantly expressed in testicular tissue (Arner and Holmgren 2006).

In this study, our objective is to assess the capacity of sodium selenite (SS), SM, or MSC in ameliorating cumulative oxidative injury associated with aging using fibroblasts as an *in vitro* cellular model.

Materials and Methods

Source and culture of primary and senescent fibroblasts

Six ampules of cryopreserved primary human neonatal dermal fibroblasts were obtained from Lonza Pharma and Bistech (Catalogue #CC-2509, Basel, Switzerland). Cells tested negative for bacteria, mycoplasma, fungi, and yeast. Monolayer confluent primary cultures were established by cultivating cells in standard Dulbecco culture medium (CM1), purchased from Thermo Fisher Scientific (Waltham, MA, USA). Cell collection, culture and subculture processes, and contents of CM1 and the trypsinization and harvesting media were previously documented (Ghneim and Al-Sheikh 2010, 2011). Senescent fibroblasts were obtained by serial subculture of CM1-cultivated primary cells up to passage 30 and fibroblasts at P5, P10, P15, P20, P25 and P30 were studied. Primary and senescent and senescent cultures were identified by measuring levels and generation rates of major oxidative stress marker including H_2O_2 , lipid peroxides (LPO), superoxide anions (SA) and total protein carbonyl content (PCC). Additionally, cells were identified by measuring the activities of key glucose and glycogen catabolic enzymes including phosphofructokinase (PFK), lactate dehydrogenase (LDH), and glycogen phosphorylase (GP).

Preparation of culture media

CM1 contained 10% fetal bovine serum (FBS) as the only source of Se totaling $0.8 \mu\text{mol/l}$. CM2, CM3, and CM4 were prepared by supplementing FBS-free CM1 with SS, SM, MSC, respectively, to give final Se concentrations of $3 \mu\text{mol/l}$ ($5 \mu\text{mol/l}$ for TrxR1). The MTT assay showed no significant cytotoxicity (Fig. S1 in Supplementary Material).

Experimental design

To identify senescent fibroblasts, PFK, LDH and GP activities as well as the levels of H_2O_2 , LPO, SA and PCC were examined in CM1-cultivated cells at P5, 10, 15, 20, 25 and 30. The CM1 medium was decanted, cells washed thoroughly with 3 ml of

sterile Hepes pH 7.2 buffer, harvested and pelleted by centrifugation at $200 \times g$ for 5 min, and appropriate sonicate aliquots used to assay parameters. To examine the effect of the different Se forms on GPx1 and TrxR activities and gene transcripts, and the levels of oxidative stress markers, CM1 of confluent cells at P5, P25 and P30 was removed, cells washed and either CM2, CM3, or CM4 (25 ml) was added and incubated with cells for 10 h. Cell sonicates were then prepared as described above and suitable aliquots were used to assay parameters. The 10-h incubation period with 3 and 5 $\mu\text{mol/l}$ of the different Se forms achieved highest activities of both GPx1 and TrxR2, respectively (Ghneim and Al-Sheikh 2011; Ghneim 2017b).

Enzyme activity assays

PFK activity was measured as detailed elsewhere (Ghneim and Al-Sheikh 2010). The method involved coupled enzyme assays which result in fructose-1,6-diphosphate and ADP formation and spectrophotometrically monitors the rate at which NADH is oxidized at 340 nm. LDH activity was determined by directly following the rate of coupled NADH formation 340 nm over a 5-min period. A standard NADH curve was constructed to establish linearity and calibrate the assay. Detailed of the reaction mixture using 100 μl of fibroblast sonicate has been documented previously (Ghneim and Al-Sheikh 2010). The GP assay was based on the determination of glucose-1-phosphate production by a set of enzymatically catalyzed reactions as is described in Ghneim and Al-Sheikh (2010). Fibroblast sonicate (25 μl) was added start the reactions and the rate of NADP reduction recorded.

TrxR1 activity determination was based on the reduction of 5,5-dithiobis-2-nitrobenzoic acid (DTNB) by NADPH to TNB that has a distinct yellow color, and the absorbance was recorded at 412 nm. A specific inhibitor, aurothiomalate, was used to assay the reduction of DTNB by TrxR1 only excluding none-thioredoxin NADPH oxidoreductases (Ghneim 2017b). GPx1 activity assay was based on the oxidation of GSH to GSSG utilizing glutathione reductase (GR) and NADPH. The decrease in NADPH absorbance, proportional to GPx1 activity, was monitored at 340 nm as NADPH was oxidized to NADP^+ (Al-Sheikh and Al-Zahrani 2018).

Oxidative stress assays

H_2O_2 production rate was measured using the fluorescent substrate AmplexTM Red (10-acetyl-3,7-dihydrophenoxazine) according to the manufacturer's protocol (ThermoFisher). In this assay, H_2O_2 oxidizes Amplex Red to produce red fluorescent resorufin measured at excitation and emission spectra of 530 and 590 nm, respectively. LPO was assayed spectrophotometrically by measuring malondialdehyde formation using thiobarbituric acid (Ghneim and Alsheibly 2016). GSH levels were quantitated using the GR-DTNB

enzymatic recycling procedure. The assay was initiated by adding glutathione to the reaction mixture and absorbance was recorded at 412 nm (Ghneim 2017a). The same reaction mixture was used to determine GSSG using a GSSG standard curve (0–10 $\mu\text{mol/l}$) in the presence of 2-vinyl pyridine for GSH derivatization. SA levels were determined by reacting with a tetrazolium salt leading to the formation of colored formazan blue which absorbs light at 450 nm (Ghneim 2017a). PCC was measured by the derivatization of protein carbonyls with 2,4-dinitrophenylhydrazine (DNPH) leading to the formation of stable dinitrophenyl hydrazone (DNP) quantitated at 375 nm (Ghneim and Alsheibly 2016).

Quantitative RT-PCR

RNA was extracted from cell pellets using Total RNA Extraction Kit (Solarbio Life Science, Beijing, China). cDNA was then synthesized from 1 μg of RNA using Solarbio's Maxima First Strand cDNA Synthesis Kit (Catalog #K1672) and amplified by qRT-PCR on iQTM5 Multicolor RT-PCR Detection System (Bio-Rad, Hercules, CA, USA) using PowerUpTM SYBRTM Green Master Mix (Applied Bioscience, Carlsbad, CA, USA) and Bio-Rad's PrimePCRTM primer pairs for *TrxR1* and *GPX1*. Relative quantification of gene expression was calculated using the $2^{-\Delta\Delta\text{CT}}$ method with *GAPDH* serving as a housekeeping gene (Alfhili et al. 2021).

Se and protein content

Se concentrations were measured in pooled CM1, CM2, CM3 and CM4 aliquots by atomic absorption spectrophotometry using appropriate wavelengths, standards, and quality control samples as detailed elsewhere (Jacobson and Lockitch 1988). Protein fibroblast content in 30 μl was assayed as is described in Bradford (1976).

Statistical analysis

Assessment of statistical differences among values recorded for different parameters at different fibroblast passages cultured in different media were calculated by ANOVA followed by *post-hoc* Dunnett's test using GraphPad Prism v9.2.0 (GraphPad Software, Inc., San Diego, CA, USA). Computed values of $p < 0.05$ were considered statistically significant.

Results

Se concentrations in culture media

The Se concentration of duplicate determination in ten pooled batches of standard medium CM1 amounted to $0.81 \pm 0.07 \mu\text{mol/l}$. The duplicate determinations of Se con-

centrations in ten pooled batches of FBS-free CM2, CM3 and CM4 media supplemented with either SS, SM or MSC equated 2.96 ± 0.28 , 3.01 ± 0.30 , and 3.04 ± 0.29 $\mu\text{mol/l}$, respectively. CM2–CM4 used for TrxR1 assays had 5.07 ± 0.43 , 5.03 ± 0.46 , and 4.99 ± 0.44 $\mu\text{mol/l}$.

Rates of DNA and protein synthesis of serial subcultures

Data regarding the rates of DNA and protein synthesis of serial subcultures in the current study are not shown to save space. However, results obtained were very similar to those reported in detail for fibroblast subcultures used by us previously (Ghneim and Al-Sheikh 2011). P5 subcultures incubated in CM1 required 24 h to achieve highest rates of (methyl ^3H) thymidine and L-(U- ^{14}C)-leucine incorporation into DNA and protein, respectively, to become confluent. In contrast, P15, P20, P25 and P30 required 48, 96 and 120 h, respectively. The same results were obtained for passages subcultured in CM2, CM3, and CM4. Consequently, different passages were harvested at their respective time of confluency, and were supplied with fresh medium when subcultured for more than 48 h.

Glucose and glycogen degradative enzyme activities

PFK, LDH, and GP specific activities did not undergo any significant changes in P5 and P10 fibroblast subcultures (Fig.

1A–C). However, beginning at P15, all enzymes exhibited significant activity increases compared to P5 cells ($p < 0.01$) amounting to ~40, 60, and 55% for PFK, LDH, and GP, respectively. Furthermore, all enzymes underwent gradual elevations in P20, P25, and P30 compared to P5 cells ($p < 0.001$) reaching highest activities at P30 equaling 76.4 ± 5.5 , 490.4 ± 42.3 , and 501.5 ± 37.8 $\mu\text{mol/min/mg}$ protein (amounting to ~260, 235, and 420% of P5 values) for PFK, LDH, and GP, respectively.

Oxidative stress markers

As illustrated in Figure 1D–G, there were no changes oxidative stress markers in P5, P10, and P15 subcultures. However, P20 cells showed significant increases ($p < 0.01$ for PCC, $p < 0.001$ for H_2O_2 , SA, and LPO compared to P5 cells). This increased generation of all markers became gradually of higher magnitude in P25 and P30 cells compared to P5 cells ($p < 0.001$ for all comparisons) and equaled in P30 5.32 ± 0.51 , 7.65 ± 0.68 , and 120.1 ± 10.5 $\mu\text{mol/min/mg}$ protein for H_2O_2 , SA, and LPO, respectively, and 12.8 ± 0.96 nmol/min/mg protein for PCC. Such increases amounted to ~230% of P5 activities for all investigate markers.

Based on of the results of all the above investigated parameters P5 fibroblasts were regarded as primary, whereas those at P25 and P30 as senescent.

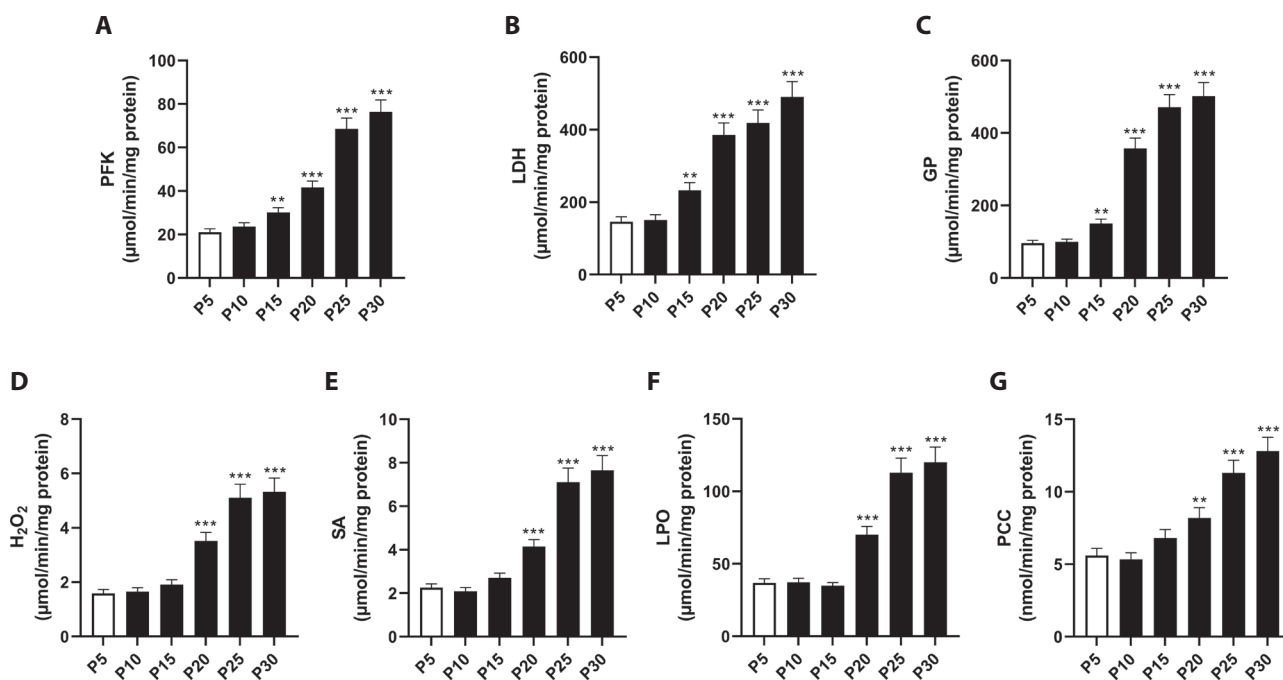


Figure 1. Senescence markers in serially subcultured fibroblasts. Enzymatic activities of PFK (A), LDH (B), and GP (C), and levels of oxidative stress markers H_2O_2 (D), SA (E), LPO (F), and PCC (G) were assayed by colorimetric methods in primary passage (P5) through senescent passage (P30) fibroblasts. Results are presented as mean percentage of control \pm SD ($n = 6$). ** $p < 0.01$, *** $p < 0.001$ vs. P5 cells.

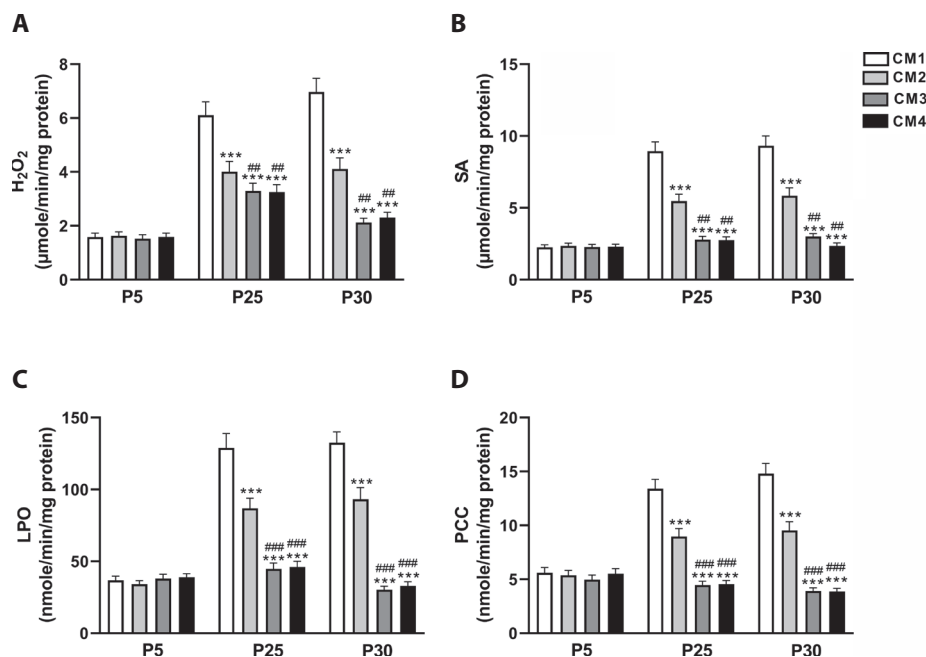


Figure 2. Alleviation of oxidative stress by Se supplementation. Levels of oxidative stress markers H₂O₂ (A), SA (B), LPO (C), and PCC (D) were measured by colorimetric assays in primary passage (P5) and senescent passage (P25 and P30) fibroblasts. Results are shown as mean \pm SD ($n = 6$). CM1 contains 10% FBS as the only source of Se (0.8 $\mu\text{mol}/\text{l}$), while CM2, CM3, and CM4 are FBS-free with SS, SM, MSC, respectively, for a total Se concentration of 3 $\mu\text{mol}/\text{l}$. *** $p < 0.001$ compared to the same passage in CM1; # $p < 0.01$, ## $p < 0.001$ compared to the same passage in CM2.

Effect of different Se forms on oxidative stress

As indicated in Figure 2, there were no variations in H₂O₂, SA, LPO, and PCC in P5 fibroblasts among CM1, CM2, CM3, and CM4. However, in senescent P25 and P30 cells, there were highly significant decreases in all investigated oxidative stress levels when the cells were incubated in CM2, CM3, or CM4 compared to CM1 ($p < 0.001$ for all comparisons). Data indicated that the decreases in all markers were higher in CM3 and CM4 compared to CM2. In CM3- and CM4-incubated P30 cells, H₂O₂ equaled 2.12 ± 0.16 and 2.31 ± 0.19 $\mu\text{mol}/\text{min}/\text{mg}$ protein, respectively, compared to 4.11 ± 0.41 $\mu\text{mol}/\text{min}/\text{mg}$ protein recorded when the cells were incubated with CM2 (Fig. 2A). In CM2-incubated P25 and P30 cells, SA generation equaled 5.47 ± 0.48 and 5.85 ± 0.55 $\mu\text{mol}/\text{min}/\text{mg}$ protein, respectively, compared to 8.95 ± 0.14 and 9.32 ± 0.68 $\mu\text{mol}/\text{min}/\text{mg}$, respectively, when the same cells were incubated in CM1 (Fig. 2B). The same pattern was exhibited by LPO (Fig. 2C) and PCC (Fig. 2D).

Effect of Se forms on the activities and gene transcripts of TrxR1 and GPx1

No significant changes were found in the activities and gene transcripts of TrxR1 and GPx1 when P5 fibroblasts were incubated in CM1, CM2, CM3, or CM4 (Fig. 3). In contrast, senescent P25 and P30 cells incubated with CM2, CM3, and CM4 exhibited very significant increases in gene expression and activities of both enzymes when compared to CM1-incubated cells.

TrxR1 gene expression was significantly higher in P25 cells incubated in CM2 (1.22 ± 0.04 folds), CM3 (1.53 ± 0.06 folds), and CM4 (1.59 ± 0.10 folds) compared to those in CM1 (1.0 ± 0.02 folds) (Fig. 3A). Similarly, this was also seen in P30 cells in CM2 (1.30 ± 0.06 folds), CM3 (1.65 ± 0.05 folds), and CM4 (1.69 ± 0.08 folds) in comparison to those in CM1 (1.01 ± 0.03 folds). The same pattern of GPx1 gene expression and activities were observed in CM2-, CM3-, and CM4-incubated P25 and P30 cells compared to those incubated in CM1. GPx1 expression significantly increased in P25 cells incubated in CM2 (1.37 ± 0.03 folds), CM3 (1.59 ± 0.06 folds), and CM4 (1.55 ± 0.04 folds) compared to CM1 (1.09 ± 0.03 folds), and in P30 cells incubated in CM2 (1.35 ± 0.04 folds), CM3 (1.64 ± 0.06 folds), and CM4 (1.66 ± 0.09 folds) compared to CM1 (1.08 ± 0.02 folds) (Fig. 3B).

Significant increases in TrxR1 activity in $\mu\text{mol}/\text{min}/\text{mg}$ protein of P25 cells equaled 39.10 ± 3.65 (CM2), 52.6 ± 4.22 (CM3), and 55.6 ± 4.30 (CM4) compared to 10.3 ± 1.01 (CM1) (Fig. 3C). In P30 cells, activities reached 47.60 ± 4.61 (CM2), 62.5 ± 4.45 (CM3), and 64.20 ± 4.88 (CM4) compared to 9.96 ± 0.84 (CM1). Figure 3D shows significant increases in GPx1 activities ($\mu\text{mol}/\text{min}/\text{mg}$ protein) of P25 cells in CM2 (4.90 ± 0.14), CM3 (5.93 ± 0.55), and CM4 (6.12 ± 0.59) compared to CM1 (2.25 ± 0.24), and of P30 cells in CM2 (6.16 ± 0.21), CM3 (7.29 ± 0.65), CM4 (7.55 ± 0.73) compared to CM1 (2.30 ± 0.22). Importantly, significantly higher TrxR1 and GPx1 gene expression ($p < 0.01$) and enzyme activities ($p < 0.05$) of P25 and P30 cells in CM3 and CM4 compared to CM2 were observed.

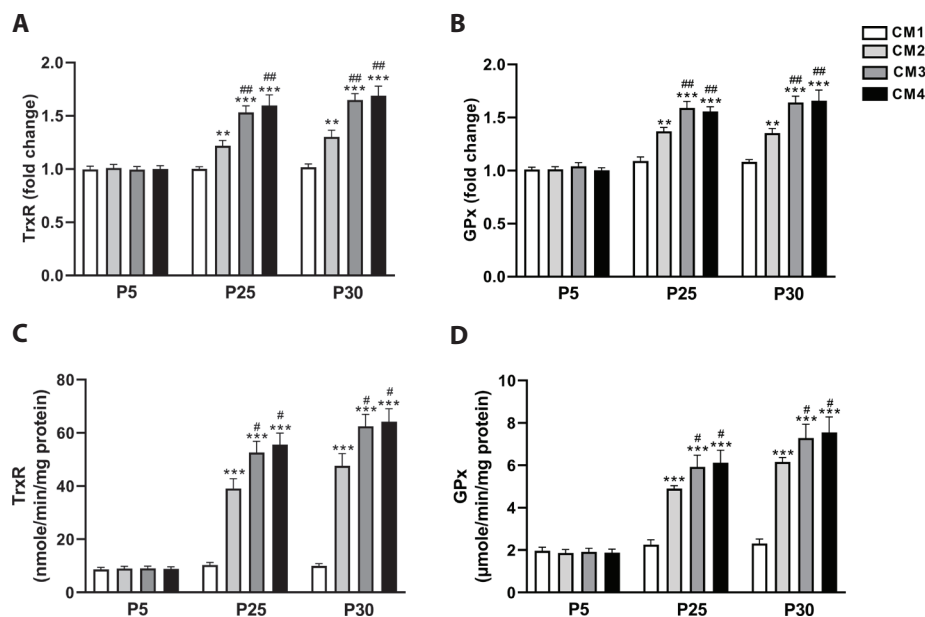


Figure 3. Effect of Se on gene expression and enzymatic activities of TrxR1 and GPx1. Transcriptional and enzymatic activities of TrxR1 (A, C) and GPx1 (B, D) in primary passage (P5) and senescent passage (P25 and P30) fibroblasts. Gene expression was detected by qRT-PCR while enzymatic activities were measured by colorimetry. CM1 contains 10% FBS as the only source of Se (0.8 $\mu\text{mol/l}$), while CM2, CM3, and CM4 are FBS-free with SS, SM, MSC, respectively, for a total Se concentration of 3 $\mu\text{mol/l}$ (5 $\mu\text{mol/l}$ for TrxR1). Results are shown as mean \pm SD ($n=6$). ** $p < 0.01$, *** $p < 0.001$ compared to the same passage in CM1; # $p < 0.05$, ## $p < 0.01$ compared to the same passage in CM2.

Effect of Se forms on glutathione status

GSH and GSSG concentrations, and the GSH/GSSG values did not undergo any changes in P5 fibroblasts cultured in CM1, CM2, CM3, or CM4 (Fig. 4). However, in CM2-cultured P25 and P35 fibroblasts, GSH and GSSG underwent moderate but significant increases and decreases, respectively, compared to levels recorded when the same cells were incubated with CM1 ($p < 0.05$ for both comparisons).

GSH levels in CM2-incubated P25 cells equaled 3.82 ± 2.78 compared to 30.8 ± 2.45 $\mu\text{mol/mg}$ protein for those incubated in CM1 (Fig. 4A), and GSSG levels equaled 1.54 ± 0.14 compared to 2.01 ± 0.18 nmol/mg protein recorded for those incubated in CM1 (Fig. 4B). However, GSH and GSSG levels in CM3- and CM4-incubated P25 and P30 cells markedly increased and decreased, respectively, compared

to CM1-incubated cells ($p < 0.001$). In CM4-incubated P30 cells, GSSG equaled 1.04 ± 0.09 against 2.42 ± 0.20 nmol/mg protein when the cells were incubated with CM1 (Fig. 4B, $p < 0.001$).

Additionally, data showed that GSH and GSSG in CM3- and CM4-incubated P25 and P30 cells were increased/decreased by more significant values compared to those incubated in CM2 ($p < 0.001$). In CM4-incubated P30 cells, increased GSH levels equaled 47.7 ± 3.22 compared to 35.9 (Fig. 4A), and GSSG decreased to 1.04 ± 0.09 compared to 1.90 ± 0.16 $\mu\text{mol/mg}$ protein in CM2-incubated cells (Fig. 4B). There were highly significant increases in GSH/GSSG ratio in CM3- and CM4-incubated P25 and P30 cells compared to those documented for CM2 ($p < 0.001$, Fig. 4C). In particular, CM3-incubated P30 cells had GSH/GSSG equal-

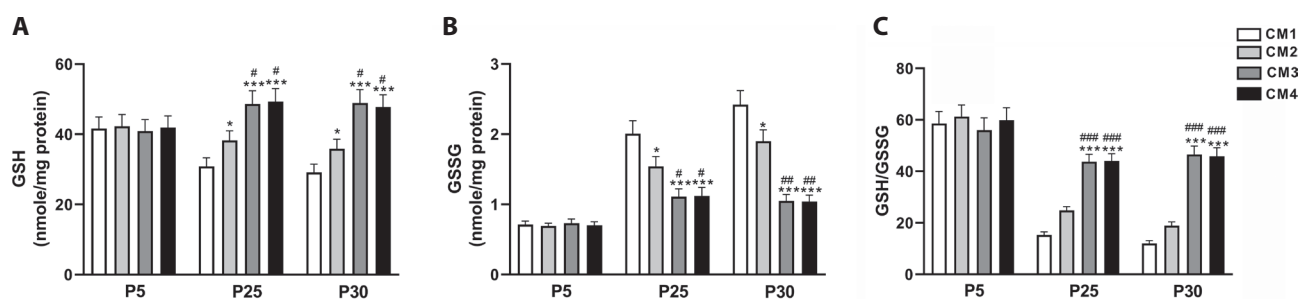


Figure 4. Improvement of glutathione status by Se forms. Levels of GSH (A) and GSSG (B), and GSH/GSSG ratio (C) were determined by the DTNB assay in primary passage (P5) and senescent passage (P25 and P30) fibroblasts. Results are shown as mean \pm SD ($n=6$). CM1 contains 10% FBS as the only source of Se (0.8 $\mu\text{mol/l}$), while CM2, CM3, and CM4 are FBS-free with SS, SM, MSC, respectively, for a total Se concentration of 3 $\mu\text{mol/l}$. * $p < 0.05$, *** $p < 0.001$ compared to the same passage in CM1; # $p < 0.05$, ## $p < 0.01$, ### $p < 0.001$ compared to the same passage in CM2.

ing 42.6 ± 3.10 compared to 18.91 ± 1.44 for CM2-incubated cells. However, such a significant GSH/GSSG increase was still significantly lower compared to those recorded for P5 cells incubated in the same medium.

Discussion

Owing to its role in regulating cellular homeostasis, research into the biochemical mechanisms governing Se action has gained grounds. As Se is offered as a dietary supplement, our results indicate that sufficient quantities are favorable to aged cells to maintain optimal antioxidant capacity and redox status to combat age-related disorders. Here, we examined the status of a comprehensive list of related parameters using serially subcultured dermal fibroblasts as an *in vitro* cellular model of aging. In contrast, previous studies examined single or few parameter(s) using different models, making our study unique.

Replicative senescence of cultured fibroblasts reflects many aspects of organismal aging, as the number of senescent cells accumulate with age (Bradford 1976; Campisi and d'Adda di Fagagna 2007). Such a model was previously employed by us to investigate metabolic changes including the lowered antioxidant capacity in senescent cells (Ghneim and Al-Sheikh 2011). Human fibroblast subcultures have a lifespan of about 40 passages (doublings), and cells were initially grown in standard culture medium (CM1) containing FBS as the sole source of Se at around the normal human plasma level. This allowed the incubation of primary and senescent subcultures with FBS-free media supplemented with different Se forms for optimal time period (10 h) and concentration previously established for achieving highest GPx1 (3 $\mu\text{mol/l}$) and TrxR1 (5 $\mu\text{mol/l}$) activities (Ghneim and Al-Sheikh 2011; Ghneim 2017b). Maximal activation and expression of key antioxidant enzymes was thus feasible, and examination of major oxidative stress and homeostatic markers was permitted. These optimal conditions also persevered the structural integrity of enzymes and enhanced proliferation of senescent cells, thus offering protection against reactive oxygen species (ROS) injury, apoptosis, and nucleic acid, protein, and lipid damage (Suzuki et al. 2012). Moreover, optimal supplemental Se concentrations modulate selenoprotein synthesis, whereas low levels decreased proliferation in culture (Combs 2015).

Replicative senescence of subcultured fibroblasts is characterized by increased activities of glucose and glycogen catabolic enzymes, increased protein oxidation, and accumulation of ROS, ultimately leading to diminished growth and replication rates (Finkel and Holbrook 2000; Campisi and d'Adda di Fagagna 2007; Ghneim and Al-Sheikh 2011; Rodier and Campisi 2011; Ghneim 2017b). Here, P5 and P10 fibroblasts subcultured in CM1 took 24 h to achieve conflu-

ence and peak rates of leucine and thymidine incorporation into protein and DNA, respectively. Nevertheless, P15 and P20 cells required 48 and 96 h, respectively, and those at P25 and P30 required 120 and 144 h, respectively (data not shown). Hence, subcultures were harvested for investigation at the above times post-incubation throughout the study. This ensured similar protein and DNA yields for all subcultures which equaled 125.6 ± 17.0 and $8.93 \pm 0.96 \mu\text{g}/100 \mu\text{l}$ sonicate, respectively, unaffected by Se concentration of the medium.

More results of the present study (Fig. 1A–C), showed very significant PFK, LDH, and GP activity increases in CM1-incubated P15 and P20 cells reaching highest magnitudes in P25 and P30 cells compared to the CM1-incubated P5 cells. Such findings are in agreement with reports, and is due to senescence and not hypoxia since cells were subcultured in an oxygen rich atmosphere (Ghneim and Al-Sheikh 2010, 2011). Additional present data (Fig. 1D–G) illustrated very significant progressive increases in levels of H_2O_2 , LPO, SA, and PCC, peaking in CM1-incubated P30 cells. This was in close agreement with those previously reported (Ghneim and Al-Sheikh 2010, 2011; Ghneim 2017b), and indicate that P5 and P10 subcultures are primary, whereas P25 and P30 are senescent.

The present results showed minimal insignificant increases in GPx1 and TrxR1 activities and gene expression levels in senescent CM1-incubated P25 and P30 cells compared to primary P5 cells incubated in the same medium. Such mild increases are probably an outcome senescence in a failed attempt to quench the high oxidative stress levels. However, current results demonstrated very marked increases in activity and upregulated expression of GPx1 and TrxR1 incubated with CM2, CM3, and CM4 containing 3 $\mu\text{mol/l}$ and 5 $\mu\text{mol/l}$ SS, SM and MSC, respectively, compared against those incubated with CM1 (Fig. 3). These findings are in agreement with previous findings were SS or SM supplementation enhanced GPx1, TrxR1 activities and expression levels, protected against LPO and SA injury and promoted Ca^{2+} signaling in endothelial cells, senescent fibroblasts, and adrenocortical cells (Hornsby et al. 1985; Zheng et al. 2005; Gupta et al. 2007; Ghneim and Al-Sheikh 2011; Watson et al. 2012). In congruence with the above results, current data also revealed that the increased ROS levels of H_2O_2 , LPO, SA, and PCC documented in CM1-subcultured senescent P25 and P30 cells were very significantly lowered in those incubated with CM2, CM3, and CM4 (Fig. 2). More interestingly, further analysis of the present data demonstrated that CM3- and CM4-incubated P25 and P30 cells underwent very significant GPx1 and TrxR1 activities increases and upregulated expression levels, coupled with very significant H_2O_2 , LPO, and PCC decreases compared to the same CM2-incubated cells. Furthermore, all the above recorded changes in CM3-incubated 25 and P30 senescent cells were

of very similar magnitudes compared to those obtained for CM4-incubated cells.

The redox cycle (GPx/GR) antioxidant system is a ROS scavenger which prevents GSH depletion and maintains intracellular redox balance (Seo et al. 2002). Present results (Fig. 4) demonstrated significant GSH level decreases and GSSG level increases in CM1-incubated senescent P25 and P30 cells compared to P5 cells subcultured in the same medium leading to a dramatically lowered GSH/GSSG ratio. The noted decrease in GSH could be caused by an unchanged GR activity, or a direct reaction of GSH with excessive H₂O₂ and SA generation by senescent cells leading to elevated GSSG levels. Alternatively, this could have been caused by a lowered activity or a downregulated expression of the *GPX1* and *TrxR1* genes responsible for GSH synthesis. Present results also indicated that in CM2-, CM3- and CM4-incubated senescent P25 and P30 cells, GSH and GSSG were significantly increased and decreased, respectively, compared to CM1-incubated cells allowing partial but significant restoration of the GSH/GSSG ratio towards normal values. Further analysis of data showed that such changes in the GSH and GSSG levels were more significant in CM3- and CM4-incubated senescent P25 and P30 cells and of similar magnitude compared to those incubated in CM2, consequently leading to much higher GSH/GSSG ratios.

There are many literature reports regarding the nature and magnitude of the antiaging effects of different Se forms in human tissues. Some showed that SM has better antiaging effects for DNA repair, and protects against UVA toxicity in human cultured fibroblasts (Seo et al. 2002; Hazane-Puch et al. 2014). In addition, organic Se forms are absorbed at a higher rate, possess greater biological activities, higher accumulation in tissues and lower toxicity (Kieliszek and Blazejak 2016; Kieliszek 2019). Another study showed that supplemental SM resulted in higher GPx1 and superoxide dismutase activities and increased plasma Se compared to SS (Sun et al. 2019). However, in a more recent study, although Se plasma levels were increased more in cows fed Se-yeast and SM compared to those fed SS, no effects on biochemical antioxidant parameters were observed (Khalili 2019).

In summary, the present study results indicated that senescent fibroblasts become more resistant to endogenous ROS in the presence of 3 µmol/l of the investigated Se forms. However, SM and MSC were more potent at alleviating ROS in those cells. One drawback of the present study was the use of triple human plasma levels (3 µmol/l) which could be toxic. Nonetheless, the percentage cell death was consistently low (~4%) regardless of the subculture passage and the Se concentration used. The normal Se plasma concentration is 0.8–1.5 µmol/l (Kipp et al. 2015), and the daily recommended allowance is 55–100 µg. Furthermore, overt cytotoxicity sets in when the dose exceeds 800 µg/day (Kieliszek and Blazejak

2016; Kieliszek 2019). Hence, the presently used 3 µmol/l and 5 µmol/l concentration is non-toxic (Fig. S1).

In conclusion, current results suggest that SM and MSC supplements are more potent for a substantive restoration of the antioxidant capacity and normal redox state compared to SS. Furthermore, present results are highly dependable since the same in-vitro human tissue model was used to assess the effect of the different Se forms on a comprehensive list of antioxidant capacity and redox state parameters.

Acknowledgment. The authors are grateful to the Deanship of Scientific Research, King Saud University for funding this research project through Vice Deanship of Scientific Research Chairs (DSRVCH); Chair of Medical and Molecular Genetics Research.

Conflict of interest. None.

References

- Al-Sheikh YA, Al-Zahrani KY (2018): The status of biochemical and molecular markers of oxidative stress in preeclamptic Saudi patients. *Curr. Mol. Med.* **18**, 475-485
<https://doi.org/10.2174/1566524019666190104105843>
- Alfhili MA, Hussein HAM, Park Y, Lee MH, Akula SM (2021): Triclosan induces apoptosis in Burkitt lymphoma-derived BJAB cells through caspase and JNK/MAPK pathways. *Apoptosis* **26**, 96-110
<https://doi.org/10.1007/s10495-020-01650-0>
- Arner ES, Holmgren A (2006): The thioredoxin system in cancer. *Semin. Cancer Biol.* **16**, 420-426
<https://doi.org/10.1016/j.semcancer.2006.10.009>
- Bradford MM (1976): A rapid and sensitive method for the quantitation of microgram quantities of protein utilizing the principle of protein-dye binding. *Anal. Biochem.* **72**, 248-254
[https://doi.org/10.1016/0003-2697\(76\)90527-3](https://doi.org/10.1016/0003-2697(76)90527-3)
- Campisi J, d'Adda di Fagnana F (2007): Cellular senescence: when bad things happen to good cells. *Nat. Rev. Mol. Cell. Biol.* **8**, 729-740
<https://doi.org/10.1038/nrm2233>
- Combs GF, Jr. (2015): Biomarkers of selenium status. *Nutrients* **7**, 2209-2236
<https://doi.org/10.3390/nu7042209>
- Ferreira RLU, Sena-Evangelista KCM, de Azevedo EP, Pinheiro FI, Cobucci RN, Pedrosa LFC (2021): Selenium in human health and gut microflora: bioavailability of selenocompounds and relationship with diseases. *Front. Nutr.* **8**, 685317
<https://doi.org/10.3389/fnut.2021.685317>
- Finkel T, Holbrook NJ (2000): Oxidants, oxidative stress and the biology of ageing. *Nature* **408**, 239-247
<https://doi.org/10.1038/35041687>
- Ghneim HK, Al-Sheikh YA (2010): The effect of aging and increasing ascorbate concentrations on respiratory chain activity in cultured human fibroblasts. *Cell. Biochem. Funct.* **28**, 283-292
<https://doi.org/10.1002/cbf.1653>
- Ghneim HK, Al-Sheikh YA (2011): Effect of selenium supplementation on glutathione peroxidase and catalase activities

- in senescent cultured human fibroblasts. *Ann. Nutr. Metab.* **59**, 127-138
<https://doi.org/10.1159/000334069>
- Ghneim HK, Alshebl MM (2016): Biochemical markers of oxidative stress in Saudi women with recurrent miscarriage. *J. Korean Med. Sci.* **31**, 98-105
<https://doi.org/10.3346/jkms.2016.31.1.98>
- Ghneim HK (2017a): The effect of *Echis coloratus* venom on biochemical and molecular markers of the antioxidant capacity in human fibroblasts. *Libyan J. Med.* **12**, 1304515
<https://doi.org/10.1080/19932820.2017.1304515>
- Ghneim HK (2017b): Selenium concentrations for maximisation of thioredoxin reductase 2 activity and upregulation of its gene transcripts in senescent human fibroblasts. *Antioxidants (Basel)* **6**, 83
<https://doi.org/10.3390/antiox6040083>
- Gouriprasanna Roy, Bani Kanta Sarma, Prasad P Phadnis, Mugesh G (2005): Selenium-containing enzyme in mammals: chemical perspectives. *J. Chem. Sci.* **117**, 287-303
<https://doi.org/10.1007/BF02708441>
- Gromer S, Eubel JK, Lee BL, Jacob J (2005): Human selenoproteins at a glance. *Cell. Mol. Life Sci.* **62**, 2414-2437
<https://doi.org/10.1007/s00018-005-5143-y>
- Gupta S, Agarwal A, Banerjee J, Alvarez JG (2007): The role of oxidative stress in spontaneous abortion and recurrent pregnancy loss: a systematic review. *Obstet. Gynecol. Surv.* **62**, 335-347
<https://doi.org/10.1097/01.ogx.0000261644.89300.df>
- Hazane-Puch F, Champelovier P, Arnaud J, Trocme C, Garrel C, Faure P, Laporte F (2014): Six-day selenium supplementation led to either UVA-photoprotection or toxic effects in human fibroblasts depending on the chemical form and dose of Se. *Metallomics* **6**, 1683-1692
<https://doi.org/10.1039/C4MT00040D>
- Hornsby PJ, Pearson DW, Autor AP, Aldern KA, Harris SE (1985): Selenium deficiency in cultured adrenocortical cells: restoration of glutathione peroxidase and resistance to hydroperoxides on addition of selenium. *J. Cell. Physiol.* **123**, 33-38
<https://doi.org/10.1002/jcp.1041230106>
- Huang JQ, Ren FZ, Jiang YY, Xiao C, Lei XG (2015): Selenoproteins protect against avian nutritional muscular dystrophy by metabolizing peroxides and regulating redox/apoptotic signaling. *Free Radic. Biol. Med.* **83**, 129-138
<https://doi.org/10.1016/j.freeradbiomed.2015.01.033>
- Jacobson BE, Lockitch G (1988): Direct determination of selenium in serum by graphite-furnace atomic absorption spectrometry with deuterium background correction and a reduced palladium modifier: age-specific reference ranges. *Clin. Chem.* **34**, 709-714
<https://doi.org/10.1093/clinchem/34.4.709>
- Khalili M, Amanlou H, Nikkah A, Sadeghi AS (2019): Effects of different sources of selenium supplementation on antioxidant indices, biochemical parameters, thyroid hormones and selenium status in transition dairy cows. *Acta Scientiarum. Animal Sciences* **41**, e44392
<https://doi.org/10.4025/actascianimsci.v41i1.44392>
- Kieliszek M (2019): Selenium(-) fascinating microelement, properties and sources in food. *Molecules* **24**, 1298
<https://doi.org/10.3390/molecules24071298>
- Kieliszek M, Bano I, Zare H (2022): A comprehensive review on selenium and its effects on human health and distribution in Middle Eastern countries. *Biol. Trace Elem. Res.* **200**, 971-987
<https://doi.org/10.1007/s12011-021-02716-z>
- Kieliszek M, Blazejak S (2016): Current knowledge on the importance of selenium in food for living organisms: A review. *Molecules* **21**, 609
<https://doi.org/10.3390/molecules21050609>
- Kieliszek M, Blazejak S, Bzducha-Wrobel A, Kot AM (2019): Effect of selenium on growth and antioxidative system of yeast cells. *Mol. Biol. Rep.* **46**, 1797-1808
<https://doi.org/10.1007/s11033-019-04630-z>
- Kieliszek M, Blazejak S, Piwowarek K, Brzezicka K (2018): Equilibrium modeling of selenium binding from aqueous solutions by *Candida utilis* ATCC 9950 yeasts. *3 Biotech.* **8**, 388
<https://doi.org/10.1007/s13205-018-1415-8>
- Kim D, Ku B, Choi EM (2020): Se-methylselenocysteine stimulates migration and antioxidant response in HaCaT keratinocytes: Implications for wound healing. *J. Trace Elem. Med. Biol.* **58**, 126426
<https://doi.org/10.1016/j.jtemb.2019.126426>
- Kipp AP, Strohm D, Brigelius-Flohe R, Schomburg L, Bechthold A, Leschik-Bonnet E, Heseker H, German Nutrition Society (2015): Revised reference values for selenium intake. *J. Trace Elem. Med. Biol.* **32**, 195-199
<https://doi.org/10.1016/j.jtemb.2015.07.005>
- Labunskyy VM, Hatfield DL, Gladyshev VN (2014): Selenoproteins: molecular pathways and physiological roles. *Physiol. Rev.* **94**, 739-777
<https://doi.org/10.1152/physrev.00039.2013>
- Legrain Y, Touat-Hamici Z, Chavatte L (2014): Interplay between selenium levels, selenoprotein expression, and replicative senescence in WI-38 human fibroblasts. *J. Biol. Chem.* **289**, 6299-6310
<https://doi.org/10.1074/jbc.M113.526863>
- Qazi IH, Angel C, Yang H, Zoidis E, Pan B, Wu Z, Ming Z, Zeng CJ, Meng Q, Han H, Zhou G (2019): Role of selenium and selenoproteins in male reproductive function: a review of past and present evidences. *Antioxidants (Basel)* **8**, 268
<https://doi.org/10.3390/antiox8080268>
- Rodier F, Campisi J (2011): Four faces of cellular senescence. *J. Cell. Biol.* **192**, 547-556
<https://doi.org/10.1083/jcb.201009094>
- Schiavon M, Pilon-Smits EA (2017): Selenium biofortification and phytoremediation phytotechnologies: a review. *J. Environ. Qual.* **46**, 10-19
<https://doi.org/10.2134/jeq2016.09.0342>
- Seo YR, Sweeney C, Smith ML (2002): Selenomethionine induction of DNA repair response in human fibroblasts. *Oncogene* **21**, 3663-3669
<https://doi.org/10.1038/sj.onc.1205468>
- Sun LL, Gao ST, Wang K, Xu JC, Sanz-Fernandez MV, Baumgard LH, Bu DP (2019): Effects of source on bioavailability of selenium, antioxidant status, and performance in lactating dairy cows during oxidative stress-inducing conditions. *J. Dairy Sci.* **102**, 311-319
<https://doi.org/10.3168/jds.2018-14974>
- Suzuki M, Suzuki K, Kodama S, Yamashita S, Watanabe M (2012): Persistent amplification of DNA damage signal involved in

- replicative senescence of normal human diploid fibroblasts. *Oxid. Med. Cell. Longev.* **2012**, 310534
<https://doi.org/10.1155/2012/310534>
- Watson M, van Leer L, Vanderlelie JJ, Perkins AV (2012): Selenium supplementation protects trophoblast cells from oxidative stress. *Placenta* **33**, 1012-1019
<https://doi.org/10.1016/j.placenta.2012.09.014>
- Zheng Y, Zhong L, Shen X (2005): Effect of selenium-supplement on the calcium signaling in human endothelial cells. *J. Cell. Physiol.* **205**, 97-106
<https://doi.org/10.1002/jcp.20378>

Received: April 19, 2022

Final version accepted: May 20, 2022

Supplementary Material

Biochemical and molecular assessment of selenium forms for the alleviation of oxidative stress in senescent human fibroblasts

Hazem K. Ghneim, Mohammad A. Alfhili , Sami O. Alharbi, Shady M. Alhusayni, Manal Abudawood and Yazeed A. Al-Sheikh

Chair of Medical and Molecular Genetics Research, Department of Clinical Laboratory Sciences, College of Applied Medical Sciences, King Saud University, Riyadh, Saudi Arabia

Supplementary Figure

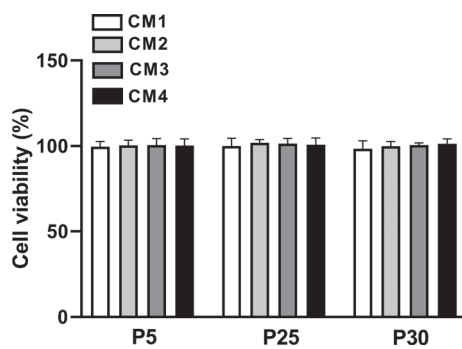


Figure S1. Cell viability. Cells were serially subcultured to induce senescence and then grown in CM1, CM2, CM3, or CM4 for 10 h at 37°C. The MTT assay was then employed to assess cell viability ($n = 6$).